A&A 386, 622–632 (2002)
DOI: 10.1051/0004-6361:20020037

Astronomy & Astrophysics

Warm molecular layers in protoplanetary disks

Y. Aikawa[1], G. J. van Zadelhoff[2], E. F. van Dishoeck[2], and E. Herbst[3]

[1] Department of Earth and Planetary Sciences, Kobe University, Kobe 657-8501, Japan
[2] Leiden Observatory, PO Box 9513, 2300 RA Leiden, The Netherlands
[3] Departments of Physics and Astronomy, The Ohio State University, Columbus, OH 43210, USA

Received 15 October 2001 / Accepted 8 January 2002

Abstract. We have investigated molecular distributions in protoplanetary disks, adopting a disk model with a temperature gradient in the vertical direction. The model produces sufficiently high abundances of gaseous CO and HCO^+ to account for line observations of T Tauri stars using a sticking probability of unity and without assuming any non-thermal desorption. In regions of radius $R \gtrsim 10$ AU, with which we are concerned, the temperature increases with increasing height from the midplane. In a warm intermediate layer, there are significant amounts of gaseous molecules owing to thermal desorption and efficient shielding of ultraviolet radiation by the flared disk. The column densities of HCN, CN, CS, H_2CO, HNC and HCO^+ obtained from our model are in good agreement with the observations of DM Tau, but are smaller than those of LkCa15. Molecular line profiles from our disk models are calculated using a 2-dimensional non-local-thermal-equilibrium (NLTE) molecular-line radiative transfer code for a direct comparison with observations. Deuterated species are included in our chemical model. The molecular D/H ratios in the model are in reasonable agreement with those observed in protoplanetary disks.

Key words. ISM: molecules – stars: pre-main sequence – stars: circumstellar matter – stars: planetary systems: protoplanetary disks

1. Introduction

It is well established from millimeter and infrared observations that the birth of solar-mass stars is accompanied by the formation of a circumstellar disk (Beckwith & Sargent 1996; Natta et al. 2000). These disks are important both as reservoirs of material to be accreted onto growing stars and as sites of planetary formation. Because the gas and dust in the disk are the basic components from which future solar systems are built, studies of their chemistry are essential to investigate the link between interstellar and planetary matter. Moreover, the chemical abundances and molecular excitation depend on physical parameters in the disks such as temperature and density, and on processes such as radial and vertical mixing. Thus, studies of the chemistry in protoplanetary disks can help to constrain their physical structure.

Although CO millimeter lines are routinely used to trace the gas and Keplerian velocity field in disks around classical T Tauri stars (e.g., Kawabe et al. 1993; Koerner et al. 1993; Dutrey et al. 1994, 1996; Koerner & Sargent 1995; Saito et al. 1995; Guilloteau & Dutrey 1998; Thi et al. 2001), detections of other molecules are still rare. Dutrey et al. (1997) and Kastner et al. (1997) were the first to report observations of molecules such as HCO^+, HCN, CN, HNC, H_2CO, and C_2H in the disks around GG Tau, DM Tau and TW Hya. Dutrey et al. found that the abundances of these species relative to hydrogen in the DM Tau and GG Tau disks are lower than those in molecular clouds by factors of 5–100 (Dutrey et al. 1994; Dutrey et al. 1997; Guilloteau et al. 1999). The abundance ratio of CN/HCN, on the other hand, is significantly higher than in molecular clouds in all three disks. More recently, Qi (2000), van Zadelhoff et al. (2001) and Thi et al. (in preparation) have reported observations of molecules other than CO in the disks around the T Tauri stars LkCa15 and TW Hya, and in those around the Herbig Ae stars MWC 480 and HD 163296, confirming the trends of high CN/HCN ratio and molecular depletion; the disk masses derived from CO (and its isotopes) are significantly smaller than those estimated from the dust continuum assuming a gas to dust ratio of 100.

Early models of the chemistry in disks considered mostly the one-dimensional radial structure in the cold midplane (e.g. Aikawa et al. 1997; Willacy et al. 1998). Subsequently, it has been recognized that the vertical stratification of the molecules is equally relevant. Aikawa & Herbst (1999a) investigated the two-dimensional chemical structure within the so-called Kyoto disk model, representative of the minimum mass solar nebula. This model has low midplane temperatures and is isothermal in the vertical direction. The molecular abundances were found

Send offprint requests to: Y. Aikawa,
e-mail: aikawa@kobe-u.ac.jp

to vary significantly with height Z from the midplane. At large radii ($R > 100$ AU), the temperature is so low that most species, except H_2 and He, are frozen out onto the grains. This depletion is most effective in the midplane region ($Z \approx 0$) because of the higher density and hence shorter timescales for molecules to collide with and stick to the grains. In regions above and below the midplane, significant amounts of molecules can remain in the gas phase for longer periods because of the lower densities, and because of non-thermal desorption by cosmic rays and/or radiation (e.g., X-rays) from the interstellar radiation field and the central star. Aikawa & Herbst (1999a) suggested that the observed molecular line emission comes mostly from this region. There is a height distinction between stable molecules and radicals, however. In the surface region of a disk, radicals such as CN are very abundant because of photodissociation via ultraviolet radiation, whereas the abundances of the stable molecules such as HCN peak closer to the midplane. The molecular column densities obtained by integrating over height at each radius compare well with those derived from observations of DM Tau (Dutrey et al. 1997), although detailed comparison through radiative transfer (i.e. calculation of molecular line intensities from model disks) is still lacking. The freeze-out of molecules in the midplane explains the low average abundances of heavy-element-containing species relative to hydrogen, whereas the high abundance ratio of CN to HCN is caused by photodissociation in the surface layers.

To obtain this good agreement with observations, Aikawa & Herbst (1999a) were forced to use the simplifying assumption that the probability S for sticking upon collision of a molecule with a grain is significantly smaller than unity. If the sticking probability is unity and if only thermal desorption is considered, the molecular column densities obtained in the Kyoto model are much smaller than observed, which suggests that either there is some efficient non-thermal desorption mechanism, or that the disk temperature is higher than assumed in the Kyoto model. Aikawa & Herbst (1999a) adopted an artificially low sticking probability $S = 0.03$ in order to reproduce the observed CO spectra, without specifying the non-thermal desorption process or modifying the temperature distribution in the Kyoto model. Since adsorption is such a dominant process in the disk, the cause of the apparently low sticking probability should be considered more seriously.

In order to explain the strong mid-infrared emission from disks, several groups suggested the possibility of higher dust temperatures than assumed in the Kyoto model due to efficient reception of stellar radiation by flared disks (e.g., Kenyon & Hartmann 1987; Chiang & Goldreich 1997; D'Alessio et al. 1998, 1999). In the two-layer Chiang & Goldreich (1997) model (C-G model hereafter), the upper layer (the so called "super-heated" layer) is directly heated by stellar radiation from the central star to temperatures $T \gtrsim 50$ K at radii of $\sim$100 AU. Also, recent observations of high-frequency lines (e.g. CO $J = 6-5$) support the possibility that the disk temperature is higher than assumed in the Kyoto model (Thi et al. 2001; van Zadelhoff et al. 2001). Willacy & Langer (2000) investigated the molecular distributions in the C-G model to see if the super-heated layer can maintain enough gaseous organic molecules to account for the observations. It was found, however, that molecules in this layer are destroyed by the harsh ultraviolet radiation from the star, whereas they are frozen out onto the grains in the cold lower layer. These authors therefore had to adopt a very high photodesorption rate in the lower layer to keep the molecules off the grains.

In this paper we report an investigation of molecular distributions in another disk model with a vertical temperature gradient: the model of D'Alessio et al. (1998, 1999). These scientists obtained the temperature and density distribution in steady accretion disks around T Tauri stars by solving the equations for local 1-D energy transfer (including radiation, convection and turbulence) and hydrostatic equilibrium in the vertical direction. Whereas in the C-G model, the disk is divided into two discrete layers – super-heated and interior – the model of D'Alessio et al. gives continuous distributions of temperature and density. The differences in the temperature and density distributions between these two models have a significant effect on the gaseous molecular abundances in the disk. Since a vertical distribution of density in the super-heated layer is not given explicitly in the C-G model, Willacy & Langer (2000) assumed a Gaussian density distribution with a scale height determined by the mid-plane temperature. In the model of D'Alessio et al., the gas is more extended than in a Gaussian distribution owing to the high temperature in the surface region. The higher densities (and thus the higher column densities) at large Z shield the lower layers from stellar ultraviolet radiation. In addition, the temperature variation in the vertical direction is more gradual in the model of D'Alessio et al. than the step function assumed in the C-G model. Therefore, compared with the C-G model, the model of D'Alessio et al. contains more gas in a warm and shielded layer, in which high abundances of gaseous molecules are expected.

The rest of the paper is organized as follows. In Sect. 2 we describe the adopted model for protoplanetary disks and the chemical reaction network. Numerical results on the distributions of molecular abundances and column densities are discussed in Sect. 3. In Sect. 4, molecular column densities and line intensities in the D'Alessio et al. model are compared with observations. Our conclusions and a discussion are given in Sect. 5.

2. Model

The disk model by D'Alessio et al. (1998, 1999) has been adopted in our work. In this model, the two-dimensional structure (R, Z) of the disk is obtained by solving for hydrostatic equilibrium and energy transport in the Z-direction. Various heating sources are considered, such as viscous dissipation of accretion energy, cosmic rays, and stellar radiation. Among them, stellar radiation is dominant at $R > 2$ AU, assuming typical

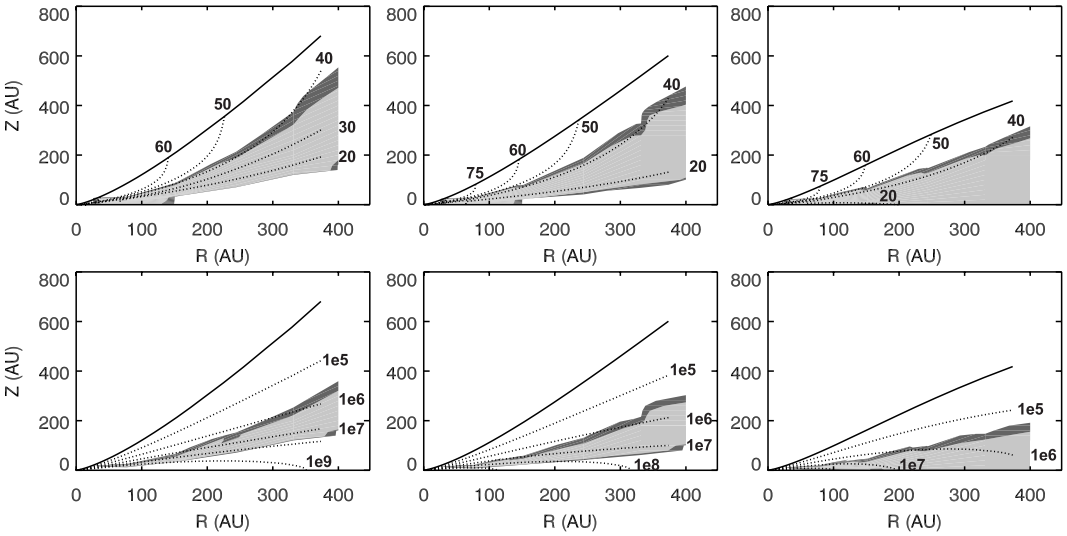

Fig. 1. The distributions of temperature T [K] (top row) and density $n(\mathrm{H_2})$ [$\mathrm{cm^{-3}}$] (bottom row) in the D'Alessio et al. model with a viscosity parameter $\alpha = 0.01$ are plotted as dotted lines. The top thick line in each panel shows the upper boundary of the model defined by $P = 10^{-10}$ dyne $\mathrm{cm^{-2}}$, which corresponds to a gas density of $n(\mathrm{H_2}) = 1.4 \times 10^4$ $\mathrm{cm^{-3}}$ with $T = 50$ K. From left to right the mass accretion rate is $10^{-7}, 10^{-8}$, and 10^{-9} $M_\odot$ $\mathrm{yr^{-1}}$, respectively. In the top row, the grey scale shows the region in which the CO abundance relative to hydrogen is 10^{-6}–10^{-5} (dark grey) and 10^{-5}–10^{-4} (light grey). In the bottom row, the fractional $\mathrm{HCO^+}$ abundance is 10^{-11}–10^{-10} (dark grey) and 10^{-10}–10^{-9} (light grey).

parameters of T Tauri stars: $T_* = 4000$ K, $M_* = 0.5$ $M_\odot$, and $R_* = 2$ $R_\odot$. We adopt a disk with an accretion rate $\dot{M} = 10^{-8}$ $M_\odot$ $\mathrm{yr^{-1}}$ and viscosity parameter $\alpha = 0.01$ as the fiducial, or standard, model, but also consider cases with the same α and differing accretion rates $\dot{M} = 10^{-7}$ $M_\odot$ $\mathrm{yr^{-1}}$ and $\dot{M} = 10^{-9}$ $M_\odot$ $\mathrm{yr^{-1}}$ (D'Alessio et al. 1999). The distributions of density and temperature in these three models are shown in Fig. 1. The surface density in the fiducial model is similar to that in the minimum-mass disk, which was adopted by Aikawa & Herbst (1999a), and is approximately an order of magnitude larger (smaller) in the model with the larger (smaller) $\dot{M}$. In the fiducial disk, the masses inside 100 AU and 373 AU are about 0.017 $M_\odot$ and 0.06 $M_\odot$, respectively.

We have selected a few radial points from the model of D'Alessio et al. (viz. $R = 26$, 49, 105, 198, 290, and 373 AU), divided the disk at each radius into several (30–40) layers, or slabs, depending on height Z, and calculated the molecular abundances in each layer as functions of time (Aikawa & Herbst 1999a). We have not included any hydrodynamic motions in the disk, such as accretion or turbulence. The main goal of this paper is to investigate the effect of a vertical temperature gradient on molecular abundances and line intensities. Although the model of D'Alessio et al. is an accretion disk model, the temperature distribution is determined by the irradiation from the central star and radiation transfer in the vertical direction, while the contribution of the accretion energy as a heat source is negligible in the region we are concerned with. In addition, we find that the chemical time scale is shorter than the accretion timescale, which is $\sim 10^6$ yr, in a large fraction of the molecular layers (Sect. 3.2), so that molecular distributions obtained in this paper can be a reasonable approximation of reality.

The chemical model and chemical reaction equations adopted in this paper are almost the same as those described in Aikawa & Herbst (2001). We use the "new standard model" for the gas-phase chemistry (Terzieva & Herbst 1998; Osamura et al. 1999), extended to include deuterium chemistry (Aikawa & Herbst 1999b). The ionization rate by cosmic rays is assumed to be the "standard" value in molecular clouds, $\zeta = 1.3 \times 10^{-17}$ $\mathrm{s^{-1}}$, because the attenuation length for cosmic-ray ionization is much larger than the column densities in the outer regions of the disks, with which we are concerned (Umebayashi & Nakano 1981). Photoprocesses induced by ultraviolet radiation from the interstellar radiation field and from the central star are included. The ultraviolet flux from the central star varies with time and object, and can reach a value 10^4 times higher than the interstellar flux at $R = 100$ AU (Herbig & Goodrich 1986; Imhoff & Appenzeller 1987; Montmerle et al. 1993). This maximum value is adopted in this paper, as in Aikawa & Herbst (1999a). We assume that the ultraviolet radiation from the central star is not energetic enough to dissociate CO and $\mathrm{H_2}$. Self- and mutual shielding of $\mathrm{H_2}$ and CO from interstellar UV is considered as in Aikawa & Herbst (1999a). Chemical processes induced by X-rays from the central star are not included in this paper.

Regarding gas-grain interactions, the surface formation of $\mathrm{H_2}$, the surface recombination of ions and electrons, and the accretion and thermal desorption of ice mantles are included, but all other grain-surface reactions are not included. The sticking probability for accretion is assumed to be 1.0, unless stated otherwise. We have not considered any modifications to the grain-surface rate equation for $\mathrm{H_2}$ formation (cf. Caselli et al. 1998), because, given our initial conditions, the rate of molecular hydrogen

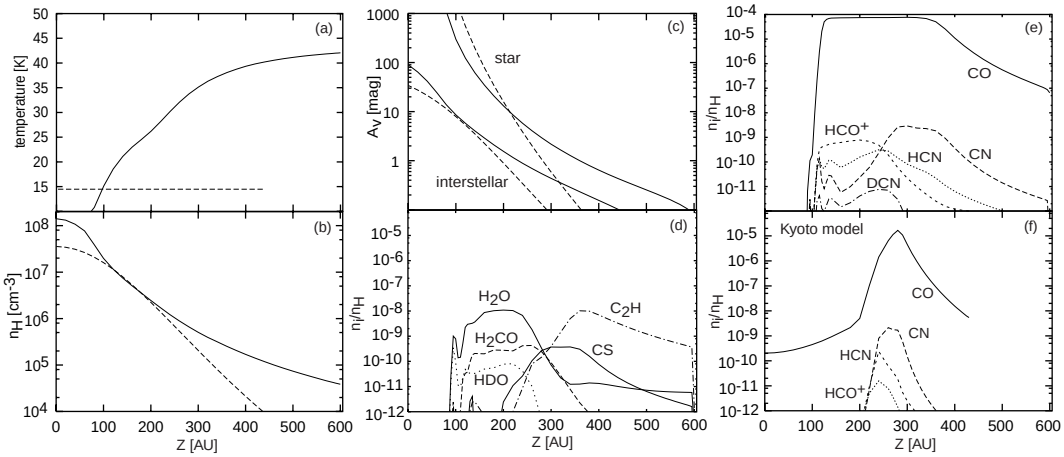

Fig. 2. Vertical distributions at $R = 373$ AU of **a)** temperature, **b)** density ($n_{\rm H} \equiv 2n({\rm H_2}) + n({\rm H})$), **c)** attenuation of the interstellar radiation ($A_{\rm v}^{\rm IS}$) and stellar radiation ($A_{\rm v}^{\rm star}$), **d–e)** molecular abundances in the D'Alessio et al. model, and **f)** molecular abundances in the Kyoto model with $S = 0.03$. In panels **a–c)**, the physical parameters of the D'Alessio et al. and Kyoto models are shown via *solid* and *dashed* lines, respectively. In panels **d–f)**, the disk age is assumed to be $t = 1.0 \times 10^6$ yr.

formation is not important to the model. The total number of species and reactions included in our network are 773 and 10 446, respectively.

The adopted elemental abundances are the so-called "low-metal" values (e.g., Lee et al. 1998; Aikawa et al. 1999). The initial molecular abundances are obtained from a model of the precursor cloud with physical conditions $n_{\rm H} = 2 \times 10^4$ cm^{-3} and $T = 10$ K at 3×10^5 yr, at which time observed abundances in pre-stellar cores such as TMC-1 are reasonably well reproduced (Terzieva & Herbst 1998).

3. Results

3.1. Vertical distribution

Figure 2 contains assorted vertical distributions at the outermost radius $R = 373$ AU in our fiducial disk model. The solid lines in Figs. 2a–c show the physical parameters: temperature, density, and $A_{\rm v}$. The attenuation of interstellar radiation ($A_{\rm v}^{\rm IS}$) is obtained from the equation

$$A_{\rm v} = \frac{N_{\rm H}}{1.59 \times 10^{21}\ {\rm cm}^{-2}}\ {\rm mag}, \qquad (1)$$

where $N_{\rm H}$ is the vertical column density of hydrogen nuclei from the disk surface to each point in the disk. The attenuation of stellar radiation ($A_{\rm v}^{\rm star}$) is obtained via the same equation, but with $N_{\rm H}$ replaced by the column density from the central star. Figures 2d–e show assorted molecular abundances at a disk age of $t = 1.0 \times 10^6$ yr, which is typical for T Tauri stars. Significant amounts of molecules exist in the gas phase due to thermal desorption at $Z \gtrsim 100$ AU, while most molecules are adsorbed onto grains below this height, where $T \lesssim 20$ K. As discussed by van Zadelhoff et al. (2001), this molecular layer covers the region in which the lines of the main isotopes of the observed species become optically thick and thus where most of the observed emission arises. The results for models with different $\dot{M}$ are similar except that the height of the molecular layer is shifted in accordance with the distribution of $A_{\rm v}^{\rm IS}$, which is the main determinant of the vertical temperature distribution.

The vertical distribution of the physical parameters (dashed lines) and molecular abundances in the Kyoto model are also shown in Figs. 2a–c, and f for comparison. The mass of the central star in the latter model is 0.5 $M_\odot$, as in the D'Alessio et al. model, so that the density distribution is modified from that adopted in Aikawa & Herbst (1999a). The sticking probability of neutral species onto grain surfaces is assumed to be 0.03, as in Aikawa & Herbst (1999a). It can be seen that the density distribution in the D'Alessio et al. model is more extended than the Gaussian profile assumed in the Kyoto model (as well as in Willacy & Langer 2000), causing more efficient ultraviolet shielding of the warm layers just below the surface. Although we have not calculated the molecular distributions in the C-G model, the width of its warm molecular layer at $R = 373$ AU can be estimated. In the C-G model, the Gaussian density distribution is similar to that in the Kyoto model, but the disk surface with $A_{\rm v}^{\rm star} \lesssim 1$ mag is "super-heated" by stellar radiation. At $R = 373$ AU, the boundary between the super-heated layer and the interior region is located at $Z \sim 280$ AU, a value estimated from the $Z - A_{\rm v}^{\rm star}$ relation in the Kyoto model (Fig. 2c). Since the temperature in the interior region is lower than 20 K at this radius in the C-G model, warm gaseous molecules exist only at heights larger than 280 AU. The upper boundary of the molecular layer, which is determined by photoprocesses, is estimated to be $Z \sim 350$ AU, again from the Kyoto model (Fig. 2f). Therefore in the C-G model, the warm molecular layer, if any, is much narrower than in the D'Alessio et al. model. This estimate is consistent with the conclusion of Willacy & Langer (2000) that they need non-thermal desorption in the cold, more shielded

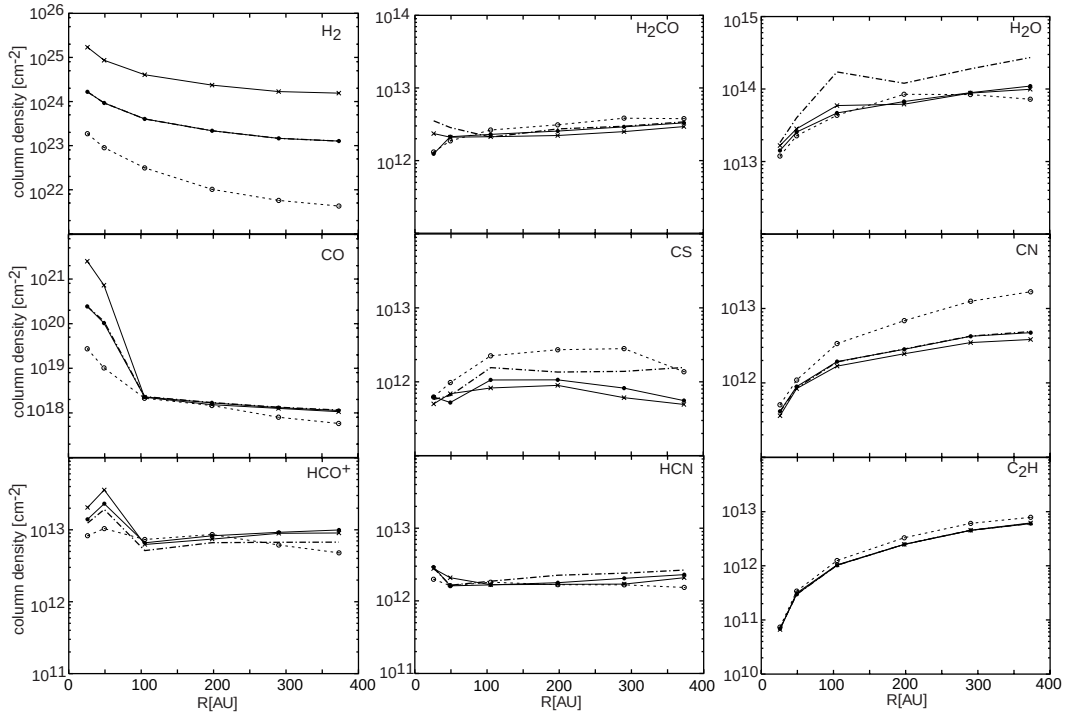

Fig. 3. The column densities of assorted molecules as functions of radius in models with mass accretion rate 1.0×10^{-7} (*solid lines with crosses*), 1.0×10^{-8} (*solid lines with closed circles*), and 1.0×10^{-9} (*dashed lines with open circles*) $M_\odot$ yr^{-1}. The viscosity parameter is fixed at $\alpha = 0.01$, while the disk age is $t = 1.0 \times 10^6$ yr. The column densities at $t = 1.0 \times 10^5$ yr in the model with mass accretion rate 1.0×10^{-8} $M_\odot$ yr^{-1} are shown with *thick dot-dashed lines*.

layer to account for the observed molecular abundances within the C-G model.

3.2. Radial distribution of column densities

Column densities are obtained by integrating the molecular abundances in the vertical direction. The column densities of assorted species as functions of disk radius are shown in Fig. 3 for three accretion disk models at $t = 1.0 \times 10^6$ yr with different mass accretion rates. Stable neutrals such as H_2CO and HCN show little dependence on radius, because these molecules are abundant only in regions with certain physical conditions and the mass contained in the layer with these physical conditions does not vary much with radius. For example, the HCN abundance is high (n(HCN)/$n_H \sim 10^{-10}$–10^{-9}) only when $n_H \lesssim 3 \times 10^7$ cm^{-3}, $T \gtrsim 20$ K, and $A_v^{IS} \gtrsim 0.2$ mag (see Fig. 2). The critical temperature of ∼20 K is not the sublimation temperature of HCN, but that of CO, which is the dominant form of carbon in the gas phase. For HCN, attenuation of interstellar radiation is more important than that of stellar radiation because the interstellar radiation penetrates deeper into the disk due to the effect of geometry. Radicals such as CN and C_2H increase in column density with radius because of the lower density and lower flux of the destructive stellar UV in the outer regions. Radical column densities are more sensitive than HCN to stellar UV, because their abundances peak at greater heights. Carbon monoxide is abundant (n(CO)/$n_H \sim 10^{-4}$) in regions with $T \gtrsim 20$ K and $A_v^{IS} \gtrsim 0.1$ mag. The column densities of CO and HCO^+ abruptly change at $R \sim 100$ AU, inside of which the temperature in the midplane is higher than 20 K. These characteristics of the radial distribution are similar to those in the Kyoto model (Aikawa et al. 1996; Aikawa & Herbst 1999a).

The amount of gas existing under physical conditions conducive for large abundances of molecules does not vary significantly among the three disk models with different accretion rates (and thus with different disk mass), either. Therefore, most (but not all) molecular column densities vary only by a very small factor among the three disk models, even though the total (H_2) column density varies by two orders of magnitude. In the model with a mass accretion rate of 1.0×10^{-9} $M_\odot$ yr^{-1}, the region with density $n_H \sim 10^5$–10^6 cm^{-3}, at which CN is abundant, is more shielded from stellar UV (Fig. 1), and thus the CN column density is higher than in the other two models.

Molecular column densities in our fiducial disk model at an earlier time of $t = 1.0 \times 10^5$ yr are shown with thick dot-dashed lines in Fig. 3. The variation in column density for most molecules during 10^5–10^6 yr is less than a factor of 2; two exceptions are CS and H_2O. In regions with A_v^{IS} smaller than a few mag, which covers a large fraction of the molecular layer, the chemical timescales are short ($\lesssim 10^5$ yr) because of photoprocesses. In the more shielded portion of the molecular layer at smaller Z, S-bearing gaseous molecules decrease in abundance after

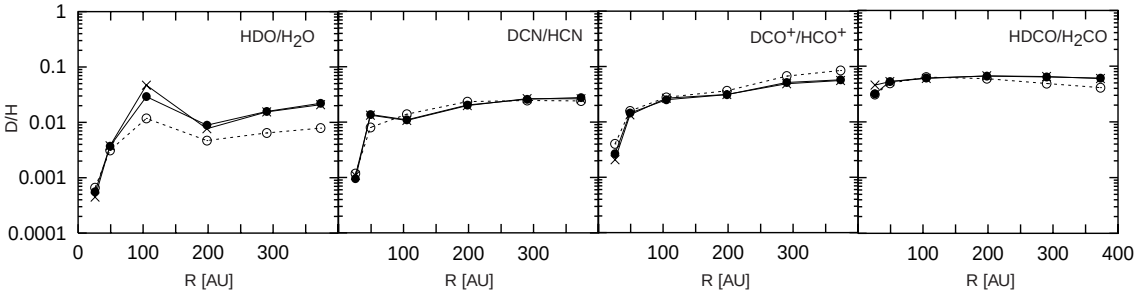

Fig. 4. Column density ratios of deuterated species to normal species as functions of radius in the three accretion disk models at an age of $t = 1.0 \times 10^6$ yr. The models are represented by the same lines as in the previous figure.

10^5 yr, since most sulfur is adsorbed onto grains in the form of CS, SO and OCS. Similarly, H_2O gas decreases at $\sim 10^6$ yr, because most oxygen which is not in CO is adsorbed as H_2O ice. On the other hand, abundances of other C-bearing molecules reach pseudo-steady-state values in a relatively short timescale ($\lesssim 10^4$ yr), and do not show significant time variation during $10^5 - 10^6$ yr in the more shielded region because CO gas, their chemical precursor, remains the dominant component of carbon for more than 1×10^6 yr. The pseudo-steady-state gas-phase chemistry of non-volatile carbon-containing species is balanced for a considerable period by formation reactions starting from CO and depletion onto the dust particles.

Values of the sticking probability S are estimated to lie in the range $0.1 \lesssim S \lesssim 1.0$ (Williams 1993, and references therein). In order to check the dependence of the molecular column densities on S, we have performed calculations with $S = 0.1$ in addition to our fiducial value of unity. Column densities of radicals such as CN and C_2H do not depend on S, because they are abundant in the surface layer, in which adsorption is not the dominant process. Among the more stable species, some show significant dependence on S; the column densities of CO_2 and OCS are larger by an order of magnitude in the model with the lower sticking probability at $R = 373$ AU and $t = 1 \times 10^6$ yr. But the effect of S is smaller for many other species; at $R = 373$ AU and $t = 1 \times 10^6$ yr, for example, the column densities of CS, HCN, and H_2CO are larger only by factors of 3.2, 1.7, and 1.3, respectively, in the case of lower S. There are two reasons for this small dependence on S. First, adsorption is not always the dominant process in the molecular layer, depending on species and height from the midplane. Second, the higher abundance of gaseous O_2 in the case of lower S reduces the abundance of the carbon atom, and thus reduces the formation rate of organic molecules, which counteracts the lower adsorption rate.

3.3. D/H ratios in molecules

In the disks around LkCa15 and TW Hya (Qi 2000, Thi et al. in preparation), the deuterated species DCN and DCO^+ have been detected, and the ratios of deuterated to normal species (DCN/HCN and DCO^+/HCO^+) are estimated to be $\sim$0.01. The deuterated species HDO has been detected in LkCa15, but there is no estimated ratio of HDO to normal water. Although the estimated ratios might include uncertainties as discussed in Sect. 4, they would not alter the important conclusion that the molecular D/H ratios are higher than the cosmic elemental abundance ratio (D/H$\approx 1.5 \times 10^{-5}$) by orders of magnitude. It is interesting to see if our model reproduces the high D/H ratios and if these ratios can be used as probes of the chemical processes and physical conditions in disks. Figure 4 shows some column density ratios of deuterated species to normal species in our models as functions of radius. The ratios are similar to the observed values of 0.01 for both HCN and HCO^+. The mechanism of deuterium enrichment in disks is similar to that in molecular clouds; due to energy differences between deuterated and normal species, molecules such as H_3^+ have a high D/H ratio, which propagates to other species through chemical reactions (Millar et al. 1989; Aikawa & Herbst 1999b; Roberts & Millar 2000). The D/H ratios decrease as the temperature rises, because the energy differences are less significant at higher temperatures. Thus, the D/H ratio decreases inwards (Fig. 4), because the temperature in the gaseous molecular layer is higher at inner radii. Because the temperature in the molecular layer does not depend much on the disk mass (see Fig. 1), the differences between models with different $\dot{M}$ are small.

The ratio of HDO/H_2O shows a more complicated behavior than described above. It has a local peak at $R \sim 100$ AU, and the peak is higher in the more massive disk model. At $R \sim 100$ AU, the midplane is at 14–16 K for the three disk models, at which temperature CO is almost completely frozen onto grains but O can marginally be kept in the gas phase to produce water vapor. The D/H ratio in the vapor is enhanced by the CO depletion in the region, since CO is one of the main destruction channels of H_2D^+ (Brown et al. 1989). The layer at this critical temperature (14 K $\lesssim T \lesssim$ 16 K) is thicker in the more massive disk. At smaller radii, the midplane temperature is higher, which lowers the D/H ratio. At larger radii for disks with $\dot{M} = 10^{-7}$ and 10^{-8} $M_\odot$ yr^{-1}, the midplane temperature is so low that O cannot remain in the gas phase to produce water vapor. The abundance of HDO has a sharp peak in a thin layer of 14 K $\lesssim T \lesssim$ 16 K offset from the midplane (Fig. 2d). In the outer disk of the $\dot{M} = 10^{-9}$ $M_\odot$ yr^{-1} model, the temperature is slightly

Table 1. Calculated ($t = 1.0 \times 10^6$ yr) molecular column densities (cm^{-2}) at $R = 373$ AU compared with observations.

Species	$\dot{M}$ [$M_\odot$ yr^{-1}]			DMTau[a]	LkCa15	
	10^{-7}	10^{-8}	10^{-9}		interferometer[b]	single dish[c]
H_2	1.5(24)[d]	1.3(23)	4.3(21)	3.8(21)		
CO	1.1(18)	1.1(18)	5.8(17)	5.7(16)[e]	1.6(18)[e]	9.0(17)[f]
HCN	2.1(12)	2.3(12)	1.5(12)	2.1(12)	0.02−1.2(15)[g]	7.8(13)
CN	3.8(12)	4.7(12)	1.7(13)	9.5−12(12)	9.1−25(13)	6.3(14)
CS	4.9(11)	5.6(11)	1.4(12)	6.5−13(11)	1.9−2.1(13)	2.2(14)
H_2CO	2.9(12)	3.3(12)	3.8(12)	7.6−19(11)		3.0−22(13)
HCO^+	9.0(12)	9.9(12)	4.8(12)	4.6−28(11)	1.5(13)	1.4(13)
C_2H	6.2(12)	6.0(12)	7.9(12)	4.2(13)		
HNC	2.0(12)	2.3(12)	1.5(12)	9.1(11)	<5.4(12)	
OCS	3.1(10)	2.8(10)	5.0(9)		<2.9(13)	
CH_3OH	6.4(8)	7.1(8)	6.6(8)		7.3−18(14)	<9.4(14)
DCN	5.5(10)	6.4(10)	3.7(10)		1.0(13)	
HDO	2.1(12)	2.4(12)	5.7(11)		2.3−6.8(14)	
N_2H^+	1.9(12)	1.9(12)	6.0(9)	<7.6(11)	<5.7(12)	<5.9(13)

[a] Derived from single-dish data by Dutrey et al. (1997) (see text).
[b] Derived from interferometer data by Qi (2000). The values in this column do not necessarily refer to 373 AU (see text).
[c] Derived from single-dish data by Thi et al. (in preparation) assuming a disk radius of 100 AU (see text).
[d] $a(b)$ means $a \times 10^b$.
[e] Estimated from $C^{18}O$ assuming $C^{16}O/C^{18}O = 500$.
[f] Estimated from ^{13}CO assuming $^{12}CO/^{13}CO = 60$.
[g] Lower value is estimated from $H^{12}CN$ and higher value is an upper limit estimated from $H^{13}CN$ assuming $H^{12}CN/H^{13}CN = 60$.

higher than 20 K even in the midplane (see Fig. 1), which causes a lower HDO/H_2O ratio than for the other two models.

4. Comparison with observation

4.1. Column densities

In the subsequent paragraphs, we discuss comparisons of our calculated column densities for assorted species at a particular radius with both single dish and interferometric data. It must be recognized, however, that it is not really possible to derive reliable columm densities at a particular radius from unresolved single dish data, making much of the subsequent discussion less quantitative than would be desirable.

Table 1 compares calculated molecular column densities obtained with three different accretion rates at a time of $t = 1.0 \times 10^6$ yr and a radius of $R = 373$ AU with those estimated from the observations of DM Tau (Dutrey et al. 1997) and LkCa15 (Qi 2000; Thi et al. in preparation). In general, it is difficult to estimate the total H_2 column density in the disk, especially at the outer radius. Dust observations suffer from uncertainties in the dust opacity at millimeter wavelengths, which depends on the grain size distribution. Moreover, the dust continuum is very weak at the outer radii and difficult to detect. The H_2 column density cannot be directly estimated from molecular lines, because the molecular abundances relative to hydrogen are not known. Therefore Dutrey et al. (1997) estimated the H_2 column density and averaged molecular abundances for DM Tau in a different way, paying attention to the critical density for excitation of the molecular lines and their optical depth. For the DM Tau disk, interferometric observations of ^{12}CO ($J = 2-1$) show that the CO gas extends to ∼800 AU from the central star. Combining the different constraints, they obtained an H_2 density $n(R, Z) = 5 \times 10^5 (R/500\ \mathrm{AU})^{-3} \exp[-(Z/H)^2]\ \mathrm{cm}^{-3}$ over this range, in which H is the scale height of the disk, with $H \approx 175$ AU at $R = 500$ AU. From the line intensities obtained in single dish telescopes, they subsequently derived molecular abundances with respect to hydrogen assuming that the abundances are constant over the entire disk. We obtained the molecular column densities of DM Tau in Table 1 by vertically integrating this disk model using the average abundances listed in Table 1 of Dutrey et al. (1997).

Although the DM Tau disk extends to about 800 AU from the central star, and the outer radius would have a larger contribution to the line intensities because of the larger surface area, we list the calculated column density at $R = 373$ AU, since the D'Alessio et al. model extends only out to this radius (the H_2 column density at $R = 800$ AU is about 3 times less than that at $R = 373$ AU in the DM Tau disk). The model with an accretion rate $\dot{M} = 10^{-9}\ M_\odot\ \mathrm{yr}^{-1}$ reproduces reasonably well the vertical H_2 column density of DM Tau, and agrees with other DM Tau observations to within a factor of 2, except for CO and C_2H. The former is overestimated, while the latter is underestimated. It should be noted that we have assumed that the stellar UV is not hard enough to dissociate CO, so that our model may overestimate the CO column density.

Inclusion of CO photodissociation by stellar UV might also increase C_2H and CN abundances, since more carbon is released from CO in the photodissociation region, in which C_2H and CN are mainly formed (van Zadelhoff et al. in preparation).

Qi (2000) performed interferometric observations on LkCa15 and estimated beam averaged molecular column densities based on the velocity-integrated intensity measured over a much smaller beam than used to determine the DM Tau abundances. The vertical column densities are lower than the listed values by a small factor, which is less than 2 if the inclination is $\lesssim$60 degrees. Since the beam size is about $0.6''-13''$ depending on the frequency of the line, the estimated values do not necessarily refer to 373 AU. If the emission is resolved and if we assume that the molecular column densities do not vary much with radius (as indicated by our disk models for $R \gtrsim 100$ AU), we can take the values listed by Qi (2000) to apply to 373 AU. The typical beam size of Qi (2000) is $3''-4''$ ($\sim$300 AU radius at the distance of LkCa15), so the majority of the results will be just resolved, making it reasonable if not perfect to compare the observations with our result at $R = 373$ AU.

In addition to the interferometric work on LkCa15, Thi et al. (in preparation) derived molecular column densities for this disk from high-frequency single dish observations of various species. Their beam-averaged values obtained with their assumption that the disk has a radius of 100 AU are included in Table 1 and differ from the interferometric column densities by up to an order of magnitude. Both values are much higher than the column densities found for DM Tau, so the agreement between our model and observations is worse for LkCa15 than for DM Tau. For CO and HCO^+ the difference is less than a factor of 2, but the column densities of other species are about 1–2 orders of magnitude higher than the model results for all three mass accretion rates. Methanol in LkCa15 appears to be a special case; its calculated column density is more than five orders of magnitude too low, presumably because it is produced by the hydrogenation of CO on grain surfaces, which is not included in our model, and then evaporated into the gas.

The use of 100 AU for LkCa15 as a reference point by Thi et al. is somewhat arbitrary. If the values obtained by Thi et al. are taken to refer to a 373 AU radius disk, their LkCa15 column densities need to be reduced by a factor $(100/373)^2$, and become closer to those found for DM Tau. Thi et al. and Qi (2000) also present data for a few other disks (TW Hya, HD 163296, and MWC 480) and determine column densities and abundances in a consistent way. Indeed, the DM Tau column densities and abundances are generally lower than the values for other disks, whereas those for LkCa15 are among the highest. Thus, these two sources appear to bracket the range of observed values.

4.2. Line intensities and profiles

In addition to the comparison with estimated molecular column densities at a single radius, a more direct comparison via line intensities from the entire model disk has been made. Since the most complete single-dish and interferometer data set is available for LkCa15, we restrict our efforts to this source. In estimating the molecular column densities from the observations, Qi (2000) assumed local thermal equilibrium (LTE) with an excitation temperature of 40 K throughout the LkCa15 disk, thereby deriving a mean column over the beam. In this paper, however, we have shown that a temperature gradient is important for the characteristics of the gaseous molecular layer in the disk and that the abundances are strongly varying with R and Z. Also, the excitation of the molecules and the line emission depend on the density structure; van Zadelhoff et al. (2001) have shown that the assumption of LTE is not always valid for high frequency lines of molecules with high critical densities. Hence, it is better to compare directly simulated line emission with observations.

We calculate here the excitation of the molecules using the 2-dimensional (2D) NLTE molecular line radiative transfer code of Hogerheijde & van der Tak (2000). From the resulting level populations, the line profiles can be computed, taking into account the inclination of the source. NLTE molecular line radiative transfer in more than one dimension has been used in star-formation research only recently (e.g., Park & Hong 1995; Juvela 1997). The need for a full treatment of the radiative transfer in disks follows from the non-locality of the problem. The level populations depend both on the local parameters (temperature, density and radiation field) and on the global radiation field, which in turn depends heavily on the optical depth of the medium. The main problem is the slow convergence of the level populations. The adopted code by Hogerheijde & van der Tak (2000) uses an accelerated Monte Carlo method to enhance convergence. A more elaborate discussion of the methods is given in van Zadelhoff et al. (2001).

The main input parameters to the radiative transfer calculations in addition to the molecular data (collision rates, Einstein A coefficients) are the 2D distributions of temperature, density and abundance of the molecule of interest at each position (R, Z). The latter is taken directly from the chemical models at a chosen age. Other important parameters are the turbulent width, taken to be 0.2 $\mathrm{km\,s^{-1}}$ (van Zadelhoff et al. 2001), the systematic Keplerian velocity field for an assumed stellar mass, the thermal line width, the size of the disk, and the inclination of the source. Qi (2000) estimates a disk inclination of $\sim 58 \pm 10$ degrees, and an outer radius of the CO disk of 435 AU for LkCa15. In the following, we assume a disk inclination of 60 degrees and a size (outer radius) of 400 AU. The dependence of line emission and profiles to disk radius and inclination can be roughly estimated (Omodaka et al. 1992; Beckwith & Sargent 1993), e.g., for optically

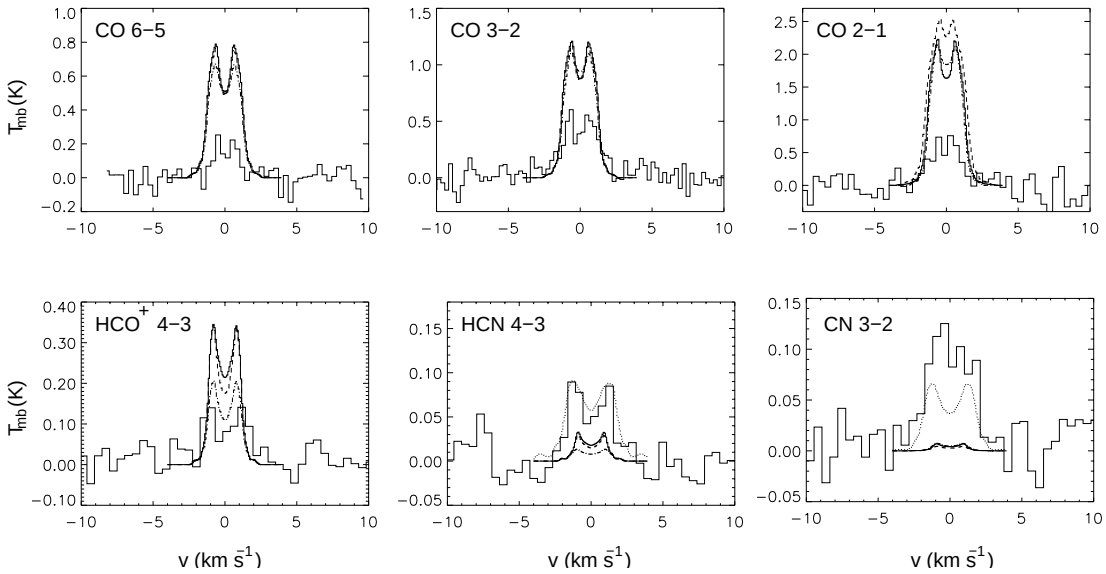

Fig. 5. Molecular line profiles from LkCa15 (*solid line*), and the D'Alessio et al. model with accretion rates of 1.0×10^{-9} (*dot-dashed line*), 1.0×10^{-8} (*thick solid line)*, and 1.0×10^{-7} (*dashed line*) $M_\odot$ yr^{-1}. The dotted line in the HCN profile represents the disk with accretion rate of 1.0×10^{-8} $M_\odot$ yr^{-1}, but HCN abundance at each position in the disk is artificially enhanced by a factor of 10 from our calculated values. Similarly, in the CN profile abundance is enhanced by a factor of 50 for the dotted line. The disk radius, age, and inclination are 400 AU, 1×10^6 yr and 60 degrees, respectively.

thick species the peak intensities of molecular lines are proportional to the square of the disk radius. Dependence of the integrated intensities on disk inclination is also discussed in van Zadelhoff et al. (2001), and is found to be less than a factor of two when the inclination is varied from 0 to 60 degree.

Figure 5 compares simulated line profiles for CO (J = 6−5, 3−2, and 2−1), HCO^+ (4−3), HCN (4−3), and CN (3−2) from the fiducial D'Alessio et al. model (thick solid line) with lines from LkCa15 observed with single-dish telescopes by van Zadelhoff et al. (2001) (solid line). Line profiles based on the D'Alessio et al. model with other accretion rates – $\dot{M} = 10^{-9}$ (dot-dashed line) and $\dot{M} = 10^{-7}$ (dashed line) $M_\odot$ yr^{-1} – are also shown. In spite of the fact that the column densities of CO and HCO^+ in our model are slightly smaller than those estimated by Qi (2000), the calculated intensities of these species are higher than observed in LkCa15 by a factor of 2−3, which is caused by the higher disk temperatures in our model. The vertical temperature gradient lowers the optical depth of the disk, which further enhances emission intensities (van Zadelhoff et al. 2001). As opposed to CO and HCO^+, the model intensities of CN and HCN are much lower than those observed in LkCa15. Those lines are optically thin in our model, and about 10 times more HCN and at least 50 times more CN are needed to fit the observed profiles, which is consistent with the comparison of column densities. The dotted lines in the CN and HCN panels show model profiles in which the molecular abundances are artificially enhanced. We conclude that CN and HCN in LkCa15 are much more abundant than in our model.

4.3. Discussion

What are the causes of the disagreement between our model results and LkCa15, and the difference between DM Tau and LkCa15? Let us first discuss the uncertainties in the estimate of the molecular column densities and size of the emission region. Although there are some differences in observed intensities, the lines in LkCa15 are, in fact, not much stronger than those in DM Tau, at most a factor of 2–3 after scaling the data to the same beam. The main reason for the different column densities in DM Tau and LkCa15 then seems to be the adopted size of the emission region, because the column densities are inversely proportional to the square of the size (radius) of the emission region. For CO, where interferometric observations have been performed both for DM Tau and LkCa15, the DM Tau disk is found to be somewhat larger than the LkCa15 disk — DM Tau is about 800 AU in radius, while LkCa15 is 435 AU. But whether this larger emission region in DM Tau holds for other species is not yet known without some degree of ambiguity because the DM Tau data come mainly from single-dish observations, and the size of the region and average molecular abundances are estimated from a model with constant abundances throughout the disk. For LkCa15, in contrast, the sizes of the emission regions are directly derived from interferometric observations and are at most a few arcseconds. Assuming that the interferometer resolves the emission, these column densities should therefore not be affected by uncertainties in the size of the emission region. Although interferometry is more direct, and thus seems more reliable for obtaining the size of the emission region, it should be noted that the derived size depends on the signal to noise ratio and dynamic range achieved in the observations.

In fact, the size of the emission region obtained via interferometry seems to contain uncertainties; the size of the CO ($J = 2-1$) emission region around LkCa15 is estimated to be ∼600 AU by Duvert et al. (2000), which is larger than the 435 AU obtained by Qi (2000).

Since our 2D modeling procedure convolves the calculated molecular emission with the actual beam of the observations, a larger disk size cannot explain the discrepancy with the LkCa15 interferometer observations, but it does affect the calculated single dish intensities. Such an increase would not be sufficient to explain the discrepancies for LkCa15, however. For example, if we assume an outer disk radius of 600 AU, the calculated HCN and CN line intensities from our model disk (Fig. 5) are increased by a factor of 2 at most, while the calculated CO and HCO^+ lines become even stronger compared with the observed profiles. There are a few possible explanations for these discrepancies. First, our model might overestimate the CO column density and underestimate the radical column density because we do not consider dissociation of CO via stellar UV radiation, as mentioned above. Detailed consideration of stellar UV radiation, including the CO and H_2 dissociation, will be reported in a forthcoming paper. Indeed, CN is enhanced by an order of magnitude depending on the treatment of the radiation field, although HCN is not much changed. The inclusion of X-rays might be another solution. X-rays cause ionization and dissociation, which enhance chemical activity, and hence increase the transformation of CO to other organic molecules such as CN and HCN (Aikawa & Herbst 1999a, 2001). Different X-ray fluxes might also account for the differing molecular column densities in DM Tau and LkCa15, if they are intrinsic. X-rays also cause non-thermal desorption, which might enhance the CN and HCN abundances in the gas phase (Najita et al. 2001). Finally, of the disks around T Tauri stars surveyed so far, LkCa15 stands out as the disk with the strongest molecular lines and richest chemistry in the interferometer and single-dish data (see Sect. 4.1, Qi 2000, Thi et al. in preparation).

5. Conclusion and discussion

We have investigated the molecular distributions in protoplanetary disks by combining the "new standard" chemical model with the physical model of D'Alessio et al., which has a temperature gradient in the vertical direction. The calculated molecular column densities are in reasonable agreement with those estimated from single-dish observations of the DM Tau disk without the assumptions in previous calculations of non-thermal desorption and/or an artificially low sticking probability. In the warmer intermediate layers of our disk models, there are large amounts of gaseous molecules owing to thermal desorption and efficient UV shielding caused by large gas densities at large heights from the midplane, a phenomenon known as flaring. Gaseous molecules are abundant only in regions with certain physical conditions. The volume of the layers with these conditions, and thus the column densities of gaseous molecules, are not proportional to the total (H_2) column density. Column densities of abundant molecules such as CN, HCN and HCO^+ do not vary by more than a factor of three during the period $t \sim 10^5-10^6$ yr. Sulfur-bearing molecules and H_2O show larger temporal variations.

Comparison of our model results with those of Willacy & Langer (2000), who adopted the C-G disk model with a Gaussian density distribution, indicates that gaseous molecular abundances are sensitive to the vertical structure of the disk model; in their model, molecules in the super-heated upper layer are destroyed by the harsh ultraviolet radiation from the star, while sufficient UV shielding is available in the warm upper layers of the D'Alessio et al. model. Deuterated species are also included in our chemical model. The molecular D/H ratios we obtain are in reasonable agreement with those observed in protoplanetary disks.

Despite our agreement with observations of DM Tau, the molecular column densities obtained in our models are smaller than those observed around LkCa15, except for CO and HCO^+. The estimated column densities of all observed molecules around LkCa15 are higher than those around DM Tau by roughly an order of magnitude. This difference in derived molecular column densities in the two objects seems to derive, at least partially, from different and/or uncertain sizes of the emission regions. Comparison with other sources shows that some of the difference is likely to be intrinsic, and other physical parameters or processes, such as X-ray ionization and dissociation, are needed to account for the high column densities in the LkCa15 disk.

In addition to the calculation of molecular abundances and column densities, we have solved the equation of radiation transfer to obtain line profiles from our model disks, which can be directly compared with observations. Such a comparison is a much more detailed test of theory than is a comparison of column densities, since line intensities depend not only on the molecular column densities but also on the density and temperature of the molecular layer and the variation of the abundance of the molecule with R and Z. The line intensities of HCN and CN obtained from the theoretical models are lower than the observed intensities in LkCa15, as expected from the comparison of column densities.

There are still several uncertainties in the vertical structure of protoplanetary disks, which might affect our results. Firstly, Chiang & Goldreich (1997) argue that the gas temperature could be lower than the dust temperature in the upper layers; although an important heat source of the gas is collisions with super-heated dust particles, gas-dust collisions are not frequent enough to equilibrate the gas temperature and grain temperature because of the low density. With a lower gas temperature, the disk would be less flared than in the model of D'Alessio et al., which assumes equal temperatures of gas and dust. Glassgold & Najita (2001) have pointed out, however, that gases in the upper layer can be heated by X-rays, which

were not considered by Chiang & Goldreich (1997). Since Glassgold & Najita (2001) have listed the temperature only in the inner radius ($R = 1$ AU), we made a rough estimate of the disk surface temperature for the outer radii $R \sim 100-300$ AU based on the work of Maloney et al. (1996), which suggests that the surface temperature of the X-ray irradiated disk is indeed higher than the midplane (interior) temperature of the C-G and Kyoto models. Moreover, the UV photons can heat the gas through the photoelectric effect on grains and PAHs, as in models of photon-dominated regions. Hence we can at least expect disks to fall off more slowly in density with increasing height than in a simple Gaussian distribution, although detailed studies on the heating and cooling balance between gas and dust are desirable in order to obtain an accurate vertical structure for the disk. Another uncertainty lies in the size and distribution of dust particles. D'Alessio et al. (2001) and Chiang et al. (2001) have noted that their original models are geometrically too thick compared with the observations of edge-on disks, which suggests dust sedimentation and/or growth in the disk. Because the molecular abundances in our model depend on the efficiency of UV shielding by "small" (i.e. interstellar) dust grains (Aikawa & Herbst 1999a), we might have overestimated these abundances. Although a more detailed approach with dust sedimentation is beyond the scope of this paper, we emphasize that molecular abundances can help to resolve uncertainties in dust evolution and disk structure.

Acknowledgements. The authors are grateful to P. D'Alessio for providing numerical tables of her models, to G. Blake, C. Qi and W. F. Thi for results of their observations prior to publication, and to M. Hogerheijde and F. van der Tak for use of their 2D Monte Carlo code. Y.A. is supported by the Grant-in-Aid for Scientific Research on Priority Areas of the Ministry of Education, Science, and Culture of Japan (13011203). Astrochemistry in Leiden is supported through a Spinoza grant from the Netherlands Organization for Scientific Research (NWO). Astrochemistry at Ohio State is supported through a grant from the National Science Foundation. Numerical calculations were carried out at the Astronomical Data Analysis Center of National Astronomical Observatory in Japan.

References

Aikawa, Y., & Herbst, E. 1999a, A&A, 351, 233
Aikawa, Y., & Herbst, E. 1999b, ApJ, 526, 314
Aikawa, Y., & Herbst, E. 2001, A&A, 371, 1007
Aikawa, Y., Miyama, S. M., Nakano, T., & Umebayashi, T. 1996, ApJ, 467, 684
Aikawa, Y., Umebayashi, T., Nakano, T., & Miyama, S. M. 1997, ApJ, 486, L51
Aikawa, Y., Umebayashi, T., Nakano, T., & Miyama, S. M. 1999, ApJ, 519, 705
Beckwith, S. V. W., & Sargent, A. I. 1993, ApJ, 402, 280
Beckwith, S. V. W., & Sargent, A. I. 1996, Nature, 383, 139
Brown, P. D., & Millar, T. J. 1989, MNRAS, 237, 661
Caselli, P., Hasegawa, T. I., & Herbst, E. 1998, ApJ, 495, 309
Chiang, E. I., & Goldreich, P. 1997, ApJ, 490, 368
Chiang, E. I., Joung, M. K., Creech-Eakman, M. J., et al. 2001, ApJ, 547, 1077
D'Alessio, P., Jorge, C., Nuria, C., & Susana, L. 1998, ApJ, 500, 411
D'Alessio, P., Nuria, C., Hartmann, L., Susana, L., & Jorge, C. 1999, ApJ, 527, 893
D'Alessio, P., Calvet, N., & Hartmann, L. 2001, ApJ, 553, 321
Dutrey, A., Guilloteau, S., & Simon, M. 1994, A&A, 286, 149
Dutrey, A., Guilloteau, S., Duvert, G., et al. 1996, A&A, 309, 493
Dutrey, A., Guilloteau, S., & Guélin, M. 1997, A&A, 317, L55
Duvert, G., Guilloteau, S., Ménard, F., Simon, M., & Dutrey, A. 2000, A&A, 355, 165
Glassgold, A. E., & Najita, J. R. 2001, in Young Stars Near Earth: Progress and Prospects, ed. R. Jayawardhana, & T. Greene, ASP Conf. Ser., in press
Guilloteau, S., & Dutrey, A. 1998, A&A, 339, 467
Guilloteau, S., Dutrey, A., & Simon, M. 1999, A&A, 348, 570
Herbig, G. H., & Goodrich, R. W. 1986, ApJ, 309, 294
Hogerheijde, M. R., & van der Tak, F. F. S. 2000, A&A, 362, 697
Imhoff, C. L., & Appenzeller, I. 1987, in Scientific Accomplishments of the I. U. E., ed. Y. Kondo (Reidel, Dordrecht), 295
Juvela, M. 1997, A&A, 322, 943
Kastner, J. H., Zuckerman, B., Weintraub, D. A., et al. 1997, Science, 277, 67
Kawabe, R., Ishiguro, M., Omodaka, T., Kitamura, Y., & Miyama, S. M. 1993, ApJ, 404, L63
Kenyon, S. J., & Hartmann, L. 1987, ApJ, 323, 714
Koerner, D. W., Sargent, A. I., & Beckwith, S. V. W. 1993, Icarus, 106, 2
Koerner, D. W., & Sargent, A. I. 1995, AJ, 109, 2138
Lee, H.-H., Roueff, E., Pineau des Forêts, G., et al. 1998, A&A, 334, 1047
Maloney, P., Hollenbach, D. J., & Tielens, A. G. G. M. 1996, ApJ, 466, 561
Millar, T. J., Bennet, A., & Herbst, E. 1989, ApJ, 340, 906
Montmerle, T., Feigelson, E. D., Bouvier, J., & André, P. 1993, in Protostars and Planets III, ed. E. H. Levy, & J. I. Lunine (Univ. of Arizona Press, Tucson), 689
Najita, J., Bergin, E. A., & Ullom, J. N. 2001, ApJ, 561, 880
Natta, A., Grinn, V., & Mannings, V. 2000, in Protostars and Planets IV, ed. A. Boss (Univ. of Arizona Press, Tucson), 559
Omodaka, T., Kitamura, Y., & Kawazoe, E. 1992, ApJ, 396, L87
Osamura, Y., Fukuzawa, K., Terzieva, R., & Herbst, E. 1999, ApJ, 519, 697
Park, Y.-S., & Hong, S. S. 1995, A&A, 300, 890
Qi, C. 2000, Ph.D. Thesis, California Institute of Technology, Pasadena, California
Roberts, H., & Millar, T. J. 2000, A&A, 361, 388
Saito, M., Kawabe, R., Ishiguru, M., et al. 1995, ApJ, 453, 384
Terzieva, R., & Herbst, E. 1998, ApJ, 501, 207
Thi, W. F., van Dishoeck, E. F., Blake, G. A., et al. 2001, ApJ, 561, 1074
Umebayashi, T., & Nakano, T. 1981, PASJ, 33, 617
van Zadelhoff, G.-J., van Dishoeck, E. F., Thi, W. F., & Blake, G. A. 2001, A&A, 377, 566
Willacy, K., Klahr, H. H., Millar, T. J., & Henning, T. H. 1998, A&A, 338, 995
Willacy, K., & Langer, W. D. 2000, ApJ, 544, 903
Williams, D. A. 1993, in ed. T. J. Millar, & D. A. Williams, Dust and Chemistry in Astronomy (Institute of Physics Publishing, London), 143